doi:10.1246/cl.2012.763
Published on the web July 14, 2012

Monodisperse Activated Carbon Spheres from Colloidal Carbon Spheres by Steam Activation and Their Electrochemical Properties

Yongjian Wu,[1,2] Quan Jin,[1,2] Chunlin Xie,[1,2] Jianghu Cui,[1,2] and Yingliang Liu*[3]
[1]*Department of Chemistry, Jinan University, Huangpu West Road 603, Guangzhou 510632, P. R. China*
[2]*Institute of Nanochemistry, Jinan University, Huangpu West Road 603, Guangzhou 510632, P. R. China*
[3]*College of Science, South China Agricultural University, Wushan Lu 483, Guangzhou 510642, P. R. China*

(Received May 17, 2012; CL-120425; E-mail: tliuyl@scau.edu.cn)

Monodisperse activated carbon spheres (ACSs) with high specific Brunauer–Emmett–Teller (BET) surface area were prepared from colloidal carbon spheres (CCSs) by steam activation. The effects of the gasification time on the surface properties of ACSs were investigated. The results exhibited that ACSs have a high specific surface area (2870 $m^2 g^{-1}$) and a large total pore volume (1.456 $cm^3 g^{-1}$). The electrochemical measurements were conducted by cyclic voltammetry. The results demonstrated that the specific capacitance of electrode material reaches 229 $F g^{-1}$ at a sweep rate of 2 $mV s^{-1}$.

In recent years, CCSs have attracted great attention for many investigators because of their potential applications, including high-density and high-strength carbon artifacts, lithium-storage materials, sacrificial templates to prepare hollow structures, coating material in core/shell structure, and catalyst support material in methanol electrooxidation.[1]

Compared with the CCSs, ACSs exhibit a higher mechanical strength, better adsorption performance, lower ash, and symmetric bulk density.[2] Many polymers have been studied as ACS precursors, such as pitch,[3a] oil-agglomerated bituminous coals,[3b] phenolic resin,[3c] divinylbenzene,[3d] and pulping black liquor.[3e] However, the ACSs synthesized from these polymers were easily adhesive or the specific BET surface area was relatively small. In this work, we prepared ACSs with good dispersity and high specific BET surface area from CCSs by steam activation. The electrochemical performances of ACSs were also investigated.

CCSs were synthesized from glucose solution by hydrothermal carbonization as described in our previous work.[4] The experimental installation of steam activation used has been described in detail elsewhere.[5] Activation of the CCSs was carried out with a horizontal tubular furnace (length of 550 mm and internal diameter of 85 mm). The reactor was an alundum tube (length of 800 mm and internal diameter of 50 mm). The CCSs were placed in the middle of the reactor and steam-activated at 900 °C (heating rate was of 5 °C min^{-1}) for 1–12 h under a nitrogen flow (80 $cm^3 min^{-1}$) saturated with steam after passing through a water saturator heated at 90 °C. After activation, the sample was cooled to ambient temperature under N_2 flow. The product was labeled as S-900-*x*, in which *x* denoted the activation time.

The morphologies were observed by scanning electron microscopy (SEM, Philips XL-30s) and transmission electron microscopy (TEM, Philips Tecnai-10). Powder XRD patterns were recorded on a MSAL-XD2 X-ray diffractometer with Cu Kα radiation (36 kV, 20 mA, $\lambda = 1.54056$ Å). The Raman spectrum was recorded at room temperature on a Renishaw RM2000 Raman microspectrometer with the 514.5 nm line of an argon laser. Nitrogen adsorption–desorption isotherms were tested using a TriStar 3000 analyzer. The electrochemical behaviors of samples were examined by cyclic voltammetry on a CHI 660B electrochemical workstation. The measurements were carried out in a standard three-electrode cell system. The working electrode was fabricated by pressing the mixture of active materials, carbon black, and 5%-poly(tetrafluoroethylene) (PTFE) (85:10:5 wt %) into a foam nickel electrode, with a nickel foil electrode as a counter electrode and a Hg/HgO (6.0 mol L^{-1} KOH) as a reference electrode, respectively.

The TEM images of the CCSs and S-900-12 are shown in Figures 1a and 1b, respectively. It shows that the ACSs still maintain their regular spherical shapes and good dispersity after steam activation, while their outer surfaces have a lot of voids and become rougher than CCSs. This is better than the case by KOH activation, by which the resulting carbon spheres were adhesive had irregular morphologies.[6] After activation, the diameter of ACSs decreases from 450 to 200 nm, which is caused by steam activation.

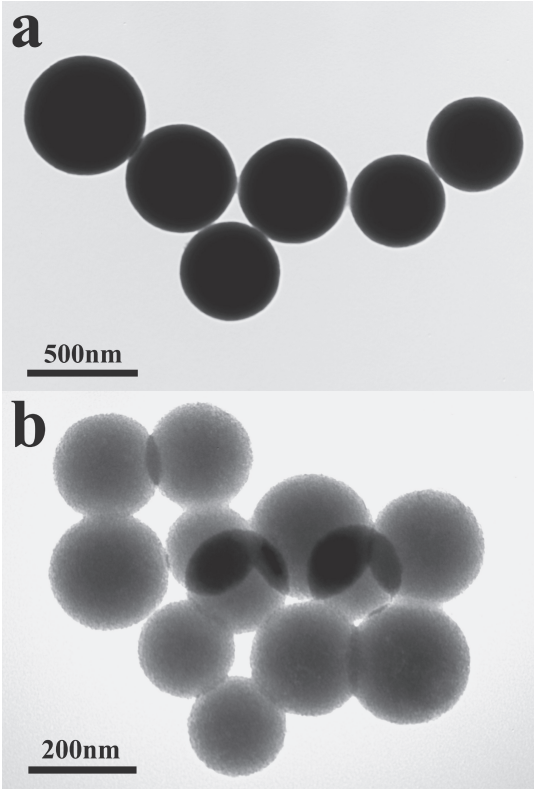

Figure 1. TEM images of the CCSs (a) and S-900-12 (b).

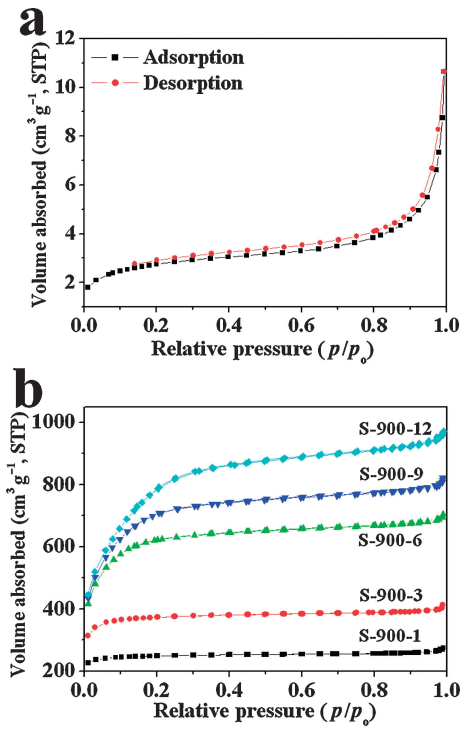

Figure 2. Adsorption–desorption isotherms of the CCSs (a) and ACSs (b).

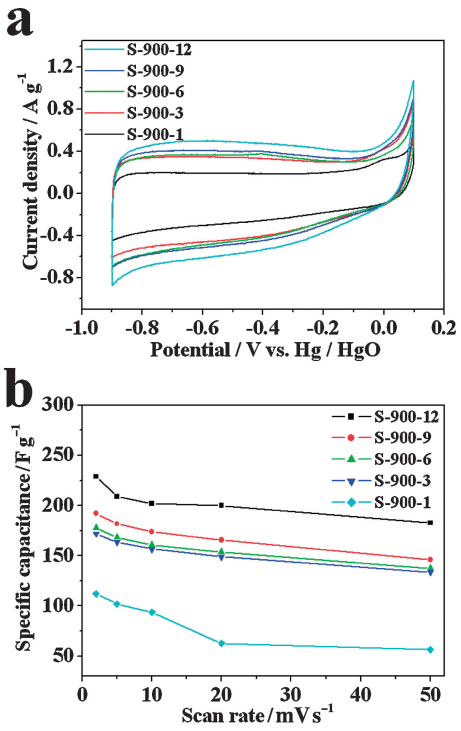

Figure 3. (a) CVs of ACSs at sweep rate of 2 mV s^{-1}, (b) the specific capacitance values of ACSs at different sweep rates.

Figure S2a[10] exhibits the XRD patterns of the prepared CCSs and S-900-12 in Supporting Information. The broad peak, which is of low peak intensity with 2θ value of 21.5°, indicates that the CCSs are amorphous in nature. After steam activation at 900 °C for 12 h, there are two peaks centered at around 21.5 and 44.0°, each corresponding to the (002) and (10) (overlapped 100 and 101) reflections of the disordered stacking of micrographites. The Raman spectrum is also used to analyze the molecular structure of the CCSs and S-900-12 (Figure S2b[10]). There are two strong peaks located within the 1590–1595 (G band) and 1340–1370 cm^{-1} (D band), respectively. It is known that the graphitization degree of carbons can be confirmed by the width of the G-band peak and the value of I_D/I_G. The value of I_D/I_G of the CCSs and S-900-12 is 0.75 and 0.94, respectively, confirming that the ACSs exhibit lower graphitized degree of order than CCSs. The relatively large I_D/I_G indicates the lower graphitized degree,[7] which shows that the CCSs and S-900-12 are disordered structures, in agreement with the XRD result.

Figure 2a shows nitrogen adsorption–desorption isotherms of the CCSs. According to the IUPAC classification, the isotherms of CCSs exhibited were type II. Specific surface area measurement reveals that the surface area for CCSs is 9.7 m^2 g^{-1}. The nitrogen adsorption–desorption isotherms of ACSs are shown in Figure 2b, which are mixed type I and IV, indicating the mesoporous character of the materials after the steam activation. The detailed surface properties parameters of the ACSs are given in Table S1.[10] It can be found that the surface areas, total pore volumes, and mesoporous volume increase steadily along with the increase of gasification time, while the pore size decreased from 5.34 to 2.85 nm. The best specific BET surface area (2870 m^2 g^{-1}) and total pore volume (1.456 cm^3 g^{-1}) are obtained when CCSs have been activated with steam at 900 °C for 12 h (S-900-12).

In order to evaluate the electrochemical characteristics of ACSs, cyclic voltammetry (CV) has been employed to characterize the electrochemical capacitance performance. Figure 3a gives the CVs of ACS electrodes at a sweep rate of 2 mV s^{-1} in 6.0 mol L^{-1} aqueous KOH solution CVs of ACSs deviate from the imaginary rectangular shape, which is due to the pseudocapacitive effects. Figure 3b shows the specific capacitance values (C) of ACS electrodes at different sweep rates. The specific capacitance of electrodes is calculated from the CVs according to the following equation:[8]

$$C = \frac{Q}{WV} = \frac{\int i\mathrm{d}t}{W\Delta V}$$

where i, W, and ΔV are the sample current, the weight of active materials, and the total potential deviation of the voltage window, respectively. The data calculated from CVs of ACSs is listed in Table S2.[10] It can be seen that the specific capacitance of ACSs increases with the increasing activation time. It is worthwhile noting that S-900-12 displays higher capacitance than the other samples. The specific capacitance of S-900-12 reaches 229 F g^{-1} at the sweep rate of 2 mV s^{-1} and improves greatly compared with S-900-1 (112 F g^{-1}). The excellent performance of S-900-12 corresponds to the higher BET surface area, larger pore volume, and higher mesoporous ratio (89.63%). The large surface area is a primary requirement for the carbon electrode materials accumulating a large amount of charges, and mesopore is advantageous to quick mass transfer and ion diffusion for aqueous capacitors, consequently, leading to a higher capacitance.[9]

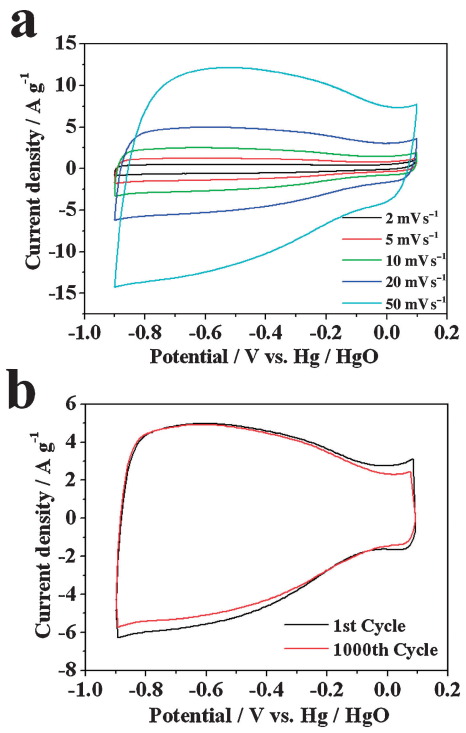

Figure 4. CVs of S-900-12 at different sweep rates (a) and at a sweep rate of 20 mV s^{-1} for 1st and 1000th cycle (b).

Figure 4a gives the CVs of S-900-12 in an aqueous KOH solution ranged from −0.9 to 0.1 V at different sweep rates. CVs of materials deviate from rectangular shape, and the reason for this may be the presence of pseudocapacitive interactions between the positively charged ions. The cyclic voltammetry experiments were performed at a sweep rate of 20 mV s^{-1} for 1000 cycles in order to investigate the cycling stability of S-900-12 (Figure 4b). It can be seen that the 1000th curve only has a slight change. The capacitance loss of S-900-12 is only 5.6% after 1000 cycles, revealing the excellent stability and reversibility of this carbon material.

In summary, we have successfully synthesized monodisperse ACSs with high specific surface area and large total pore volume from CCSs through steam activation. Activation time plays an important role in determining the surface areas and porosities of the resulting ACSs. The surface area and pore volume of S-900-12 are 2870 $m^2 g^{-1}$ and 1.456 $cm^3 g^{-1}$ respectively. The specific capacitance of S-900-12 is as high as 229 F g^{-1} at the sweep rate of 2 mV s^{-1}, which also possesses excellent stability and reversibility. The excellent performance makes the synthesized ACSs promising electrode materials for the applications of supercapacitors.

This work was financially supported by the National Nature Science Foundation of China (Nos. 21031001, U0734005, and 20906037), and the Fundamental Research Funds for the Central Universities (No. 21610102).

References and Notes

1 C. Chen, X. Sun, X. Jiang, D. Niu, A. Yu, Z. Liu, J. Li, *Nanoscale Res. Lett.* **2009**, *4*, 971.
2 C. Liu, X. Liang, X. Liu, Q. Wang, L. Zhan, R. Zhang, W. Qiao, L. Ling, *Appl. Surf. Sci.* **2008**, *254*, 6701.
3 a) Z. Wang, L. Zhan, M. Ge, F. Xie, Y. Wang, W. Qiao, X. Liang, L. Ling, *Chem. Eng. Sci.* **2011**, *66*, 5504. b) G. Gryglewicz, K. Grabas, E. Lorenc-Grabowska, *Carbon* **2002**, *40*, 2403. c) Y. Liu, K. Li, J. Wang, G. Sun, C. Sun, *J. Mater. Sci.* **2009**, *44*, 4750. d) Z. Zhu, A. Li, L. Yan, F. Liu, Q. Zhang, *J. Colloid Interface Sci.* **2007**, *316*, 628. e) J. Zhang, L. Yu, Z. Wang, Y. Tian, Y. Qu, Y. Wang, J. Li, H. Liu, *J. Chem. Technol. Biotechnol.* **2011**, *86*, 1177.
4 Y. Wu, M. Zheng, C. Xie, Q. Jin, G. Yi, Y. Liu, *Chin. J. Inorg. Chem.* **2011**, *12*, 2447.
5 C. Bouchelta, M. S. Medjram, O. Bertrand, J.-P. Bellat, *J. Anal. Appl. Pyrolysis* **2008**, *82*, 70.
6 M. Li, W. Li, S. Liu, *Carbohydr. Res.* **2011**, *346*, 999.
7 M. Huang, X. Ju, C. Wang, Y. Tang, X. Jiang, *Chem. Lett.* **2009**, *38*, 816.
8 T. Zhou, S. Mo, S. Zhou, W. Zou, Y. Liu, D. Yuan, *J. Mater. Sci.* **2011**, *46*, 3337.
9 D.-s. Yuan, T.-x. Zhou, S.-l. Zhou, W.-j. Zou, S.-s. Mo, N.-n. Xia, *Electrochem. Commun.* **2011**, *13*, 242.
10 Supporting Information is available electronically on the CSJ-Journal Web site, http://www.csj.jp/journals/chem-lett/index.html.

